AD-A132 908 MULTIWAVELENGTH BIDIRECTIONAL COUPLER-DECOUPLERS(U) 1/1
HUGHES RESEARCH LABS MALIBU CA J MYER ET AL. MAY 83
CECOM-82-C-J071-2 DAAB07-82-C-J071

UNCLASSIFIED F/G 20/6 NL

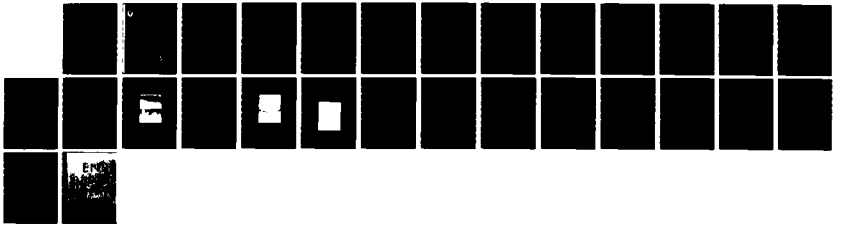

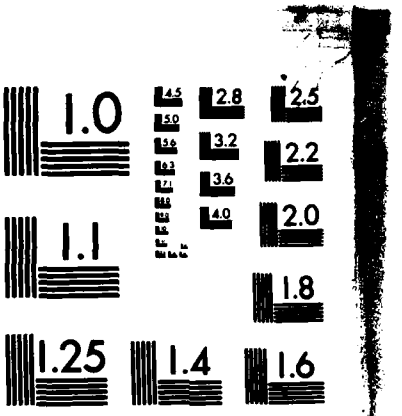

RESEARCH AND DEVELOPMENT TECHNICAL REPORT
DAAB07-82-C-J071

MULTIWAVELENGTH BIDIRECTIONAL COUPLER-DECOUPLERS

J. MYER AND H.W. YEN

Hughes Research Laboratories
3011 Malibu Canyon Road
Malibu, CA 90265

MAY 1983

INTERIM REPORT NO. 2 FOR PERIOD
1 NOVEMBER 1982 – 30 APRIL 1983

CECOM
U S ARMY COMMUNICATIONS-ELECTRONICS COMMAND
FORT MONMOUTH, NEW JERSEY 07703

NOTICES

Disclaimers

The citation of trade names and names of manufacturers in this report is not to be construed as official Government indorsement or approval of commercial products or services referenced herein.

Disposition

Destroy this report when it is no longer needed. Do not return it to the originator.

UNCLASSIFIED

SECURITY CLASSIFICATION OF THIS PAGE (When Data Entered)

REPORT DOCUMENTATION PAGE		READ INSTRUCTIONS BEFORE COMPLETING FORM
1. REPORT NUMBER CECOM-82-C-J071-2	2. GOVT ACCESSION NO.	3. RECIPIENT'S CATALOG NUMBER
4. TITLE (and Subtitle) Multiwavelength Bidirectional Coupler-Decoupler		5. TYPE OF REPORT & PERIOD COVERED Interim Report No. 2 1 Nov 82 - 30 Apr 83
		6. PERFORMING ORG. REPORT NUMBER
7. AUTHOR(s) Jon Myer and H.W. Yen		8. CONTRACT OR GRANT NUMBER(s) DAAB07-82-C-J071
9. PERFORMING ORGANIZATION NAME AND ADDRESS Hughes Research Laboratories 3011 Malibu Canyon Road Malibu, CA 90265		10. PROGRAM ELEMENT, PROJECT, TASK AREA & WORK UNIT NUMBERS 1L1 62701 AH 92
11. CONTROLLING OFFICE NAME AND ADDRESS US Army CECOM ATTN: DRSEL-COM-RM-1 Fort Monmouth, NJ 07703		12. REPORT DATE May 1983
		13. NUMBER OF PAGES
14. MONITORING AGENCY NAME & ADDRESS(if different from Controlling Office) US ARMY CECOM ATTN: DRSEL-COM-RM-1 Fort Monmouth, NJ 07703		15. SECURITY CLASS. (of this report) UNCLASSIFIED
		15a. DECLASSIFICATION/DOWNGRADING SCHEDULE

16. DISTRIBUTION STATEMENT (of this Report)

Approved for public release; distribution unlimited.

17. DISTRIBUTION STATEMENT (of the abstract entered in Block 20, if different from Report)

Approved for public release; distribution unlimited.

18. SUPPLEMENTARY NOTES

N/A

19. KEY WORDS (Continue on reverse side if necessary and identify by block number)

Multiwavelength Coupler-Decoupler
Wavelength Division Multiplexer
Fiber Optic Coupler

20. ABSTRACT (Continue on reverse side if necessary and identify by block number)

This is an exploratory program to develop, fabricate and test a family of active and passive, single and two-fiber, fiber optic multiwavelength, bidirectional, coupler-decoupler modules. The goal of the contract is to have each member of the coupler-decoupler (multiplexer-demultiplexer) family be capable of coupling energy into, and decoupling energy out of, a single optical transmission line, using a minimum of four wavelengths for the simultaneous full duplex transmission of a minimum of

DD FORM 1 JAN 73 1473 EDITION OF 1 NOV 65 IS OBSOLETE UNCLASSIFIED

SECURITY CLASSIFICATION OF THIS PAGE (When Data Entered)

20. ABSTRACT

four optical channels. The coupler-decoupler will be designed for low throughput loss (<5 dB per channel, per single pass) and minimum crosstalk (no more than -35 dB of the received optical signal). The modules fabricated during the program will be evaluated for their ability to meet military environmental requirements, particularly with respect to temperature. The approach uses the miniature planar Rowland spectrometer configuration recently developed at Hughes Research Laboratories (HRL) for NASA as the basic building block for constructing the coupler-decoupler required for this program, eliminating the need for collimating optics, prisms, or thin-film filters.

TABLE OF CONTENTS

LIST OF ILLUSTRATIONS

SECTION I

INTRODUCTION AND SUMMARY

Recent progress in the manufacture of optical fibers with a wide low-loss spectral window of 0.8 to 1.6 μm and of low-threshold, long-life semiconductor light sources covering the corresponding wavelength region has made wavelength division multiplexing (WDM) possible. The WDM technique effectively provides multiple transmission channels using a single optical fiber and enables the optical fiber to be used more efficiently. Therefore, this technique is expected to increase the information capacity of a single optical fiber by realizing full duplex transmission of various types of digital and analog modulated signals.

For a WDM system, a coupler (multiplexer) and a decoupler (demultiplexer) are necessary for the transmitter and the receiver, respectively. A multiplexer consists of input fibers (each coupled to a source of a specific wavelength), a multiplexing circuit, and a transmission fiber. A demultiplexer consists of a transmission fiber, a demultiplexing circuit, and output fibers. A multiplexing circuit couples optical signals of different wavelengths to a single transmission fiber, and a demultiplexer circuit separates these optical multiple signals.

The present contract is an exploratory development program to develop, fabricate, and test a family of fiber optic, multiwavelength, bidirectional coupler-decoupler modules that can provide simultaneous full duplex transmission of a minimum of four channels over either a two-fiber or a single-fiber line. The coupler-decouplers should have low throughput loss (<5 dB per channel, per single pass) and minimum crosstalk (< -35 dB of the received optical signal).

Our approach to the coupler-decoupler design uses a miniature planar waveguide Rowland spectrometer configuration as the basic building block. The geometry of the Rowland device is

shown in Figure 1. The structure consists of a low-loss planar optical waveguide with a pair of cylindrical surfaces. The back surface, which supports a reflection grating, has a radius of curvature, R. The opposite surface, to which the input and output fibers are attached, is located a distance, R, away from the grating and has a radius of curvative, R/2. The Rowland spectrometer combines the operation of a diffraction grating with a concave mirror to achieve spectral point-to-point imaging. By the incorporation of a planar waveguide, optical radiation is essentially confined to a two-dimensional plane, which eases the fiber alignment problem while enhancing the durability of the structure.

During the first six months of the program, as reported in the first semiannual report, we reviewed the basic design of the coupler-decoupler modules and have completed the mechanical construction of the test set structure that houses the waveguide, the detectors and the lasers. We have identified a central flaw layer in thin, hot-formed commercial glass sheets used as the guiding layers of the Rowland devices that may create severe aberration problems. Consequently, we developed a grinding and polishing process so that thicker glass sheets can be used and so that the flaw layer is polished away in the final guiding structure. We have also completed the fabrication of precise master laps required to prepare the cylindrical ends of the Rowland module. In addition, a number of solutions were developed for technical problems that were encountered during the waveguide fabrication process, including the cementing of glass layers.

During the second half-year of the program we developed a laminating process (patent disclosure submitted) for forming a reliable bond of optical quality and low refractive index (n_d = 1.463). The excellent mechanical strength of this bond aggravates the effects of thermal coefficient of expansion mismatch between the core glass layer and the cladding glass

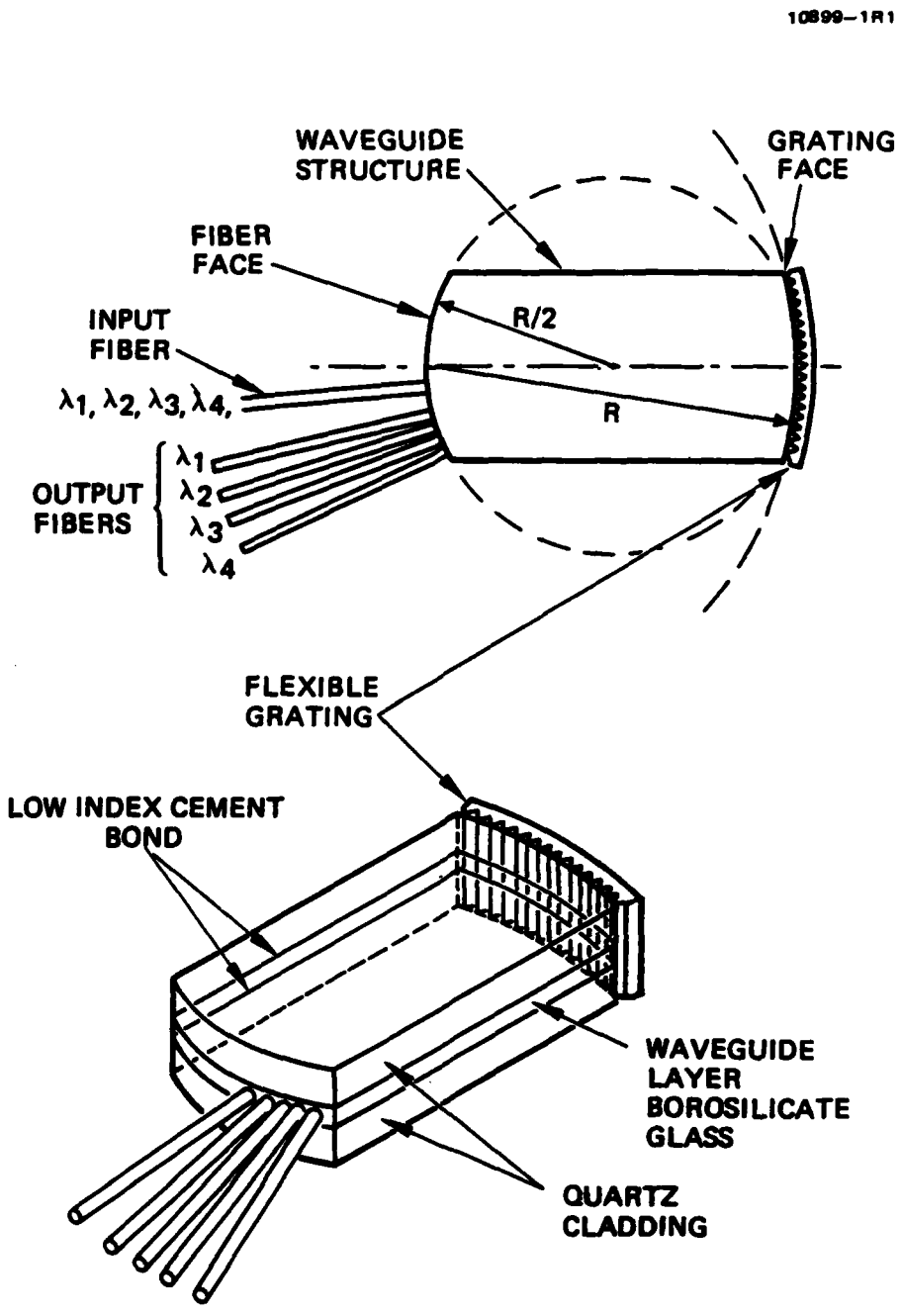

Figure 1. Planar waveguide Rowland coupler-decoupler.

layer of the planar waveguide. Component glasses of our previously selected pair had been chosen for optical properties alone, with no consideration for their thermomechanical properties. The core glass was selected for its low index in order to reduce Fresnel losses at the fiber-to-planar waveguide transition, and the cladding glass was selected for an index that would provide the best numerical aperture match. As a result, the thin borosilicate core glass layer, with its much larger thermal coefficient of expansion than that of the thick quartz layer, is under great tensile stress during cooling after hot laminating. Excellent adhesion and the large coefficient mismatch combine to generate tensile forces which are large enough to rupture the thin core layer. It now appears that the "total destruction" of the core layer during grinding and polishing (see page 16 of first intermediate report) and the ultimate rupture of even successfully polished layers was caused by this effect.

The requirement to match coefficients of thermal expansion has therefore been added to the specifications of the two planar waveguide glasses. To date, we have not found a glass pair with the ideal combination of low index core glass, a pair numerical aperture of 0.2, and a matching coefficient of thermal expansion. However, a pair of glasses with approximately the desired properties was selected and ordered. In this pair the thin core layer will be under compression after cooling which should eliminate the tensile rupture problem.

Work continues on the holographic formation of blazed gratings on single crystal silicon wafers. A new, simple and promising alternate approach to the formation of short focal length gratings has been found with the help of our supplier of ruled gratings. We were able to obtain ruled, blazed precision replica gratings on flexible microscope cover glass substrates. Early experiments on these gratings show efficiencies in excess of 70% and good channel separation. Low cost is an attractive feature of these thin replica gratings.

SECTION II

FABRICATION AND EVALUATION OF BLAZED GRATINGS

The concave diffraction grating is the wavelength dispersive element in our coupler-decouplers. In order to achieve low overall insertion loss of the coupler-decoupler modules, an efficient grating is essential. For maximum grating efficiency, a properly blazed grating should be used. However, as pointed out in our last interim report, the small radius of curvature of the device makes it difficult to fabricate an efficient grating by direct ruling.

As an alternative, we have investigated the possibility of using thin, single-crystal silicon platelets of suitable orientation to fabricate blazed gratings by anisotropic chemical etching through a holographically generated grating mask. These grating platelets are then bent to conform to the miniature Rowland geometry of the coupler-decouplers.

We have also studied blazed planar replica gratings on thin, flexible substrates. These gratings have the advantage of relatively low cost and high efficiency. They can be bent to the desired radius of curvature as well.

A. SINGLE CRYSTAL SILICON GRATINGS

Silicon has a diamond crystal structure and its chemical etch rate in the (100) direction is greater than the (110) direction, which in turn is much greater (approximately 400:1) than the (111) direction. The fabrication process basically involves slicing a single-crystal silicon substrate wafer with the proper crystal orientation to achieve a particular grating shape or blaze angle. A SiO_2 layer is thermally grown onto the substrate to serve as a mask for the chemical etching. Initially, lithographic patterning of the grating is done in a photoresist layer coated on the oxide; then the pattern is

transferred into the oxide by acid etching or by reactive plasma etching. The substrate is then exposed to a chemical etchant, such as potassium hydroxide (KOH), which preferentially etches along certain crystalline directions. This technique can be used to fabricate both symmetric grating profiles and well-controlled blazed profiles.

For example, if the grating mask is aligned along a (110) direction of a (100) silicon slice (Figure 2), V-shaped grooves are produced with smooth (111) walls. The etch progresses in the (100) direction and is terminated at a depth of 0.707 of the oxide opening width, where the etch front meets the (111) planes, intersecting the (100) plane at the edge of the mask opening. The apex angle of the groove is 109.47°. To fabricate blazed diffraction gratings, the single crystal silicon substrate wafer can be cut and polished to achieve the desired blazed angle, as shown in Figure 2. Note that apex angles of either 109.47° or 70.53° are attainable, depending on the chosen crystal orientation.

Blazed gratings thus fabricated inevitably have a flat top defect that is caused by the etching mask protecting a portion of the substrate surface. While a true blazed grating has a maximum diffraction efficiency of 100%, the flat top defect could lower the attainable maximum diffraction efficiency substantially.

During this reporting period we carried out a series of experiments to determine the process variables. For the first experiment we obtained a single crystal silicon ingot of ~1 in. diameter with <111> crystal axis. The ingot was oriented using X-ray diffraction data to the desired 9° blaze angle. It was then sliced and polished to a mirror finish. The wafers were oxidized with a 2000 to 3000-Å oxide layer, coated with photoresist and exposed to a laser interference fringe pattern. For our initial trial, the grating period was chosen to be ~9 μm so that most of the process parameters could be determined without the complication of small line spacing. We determined

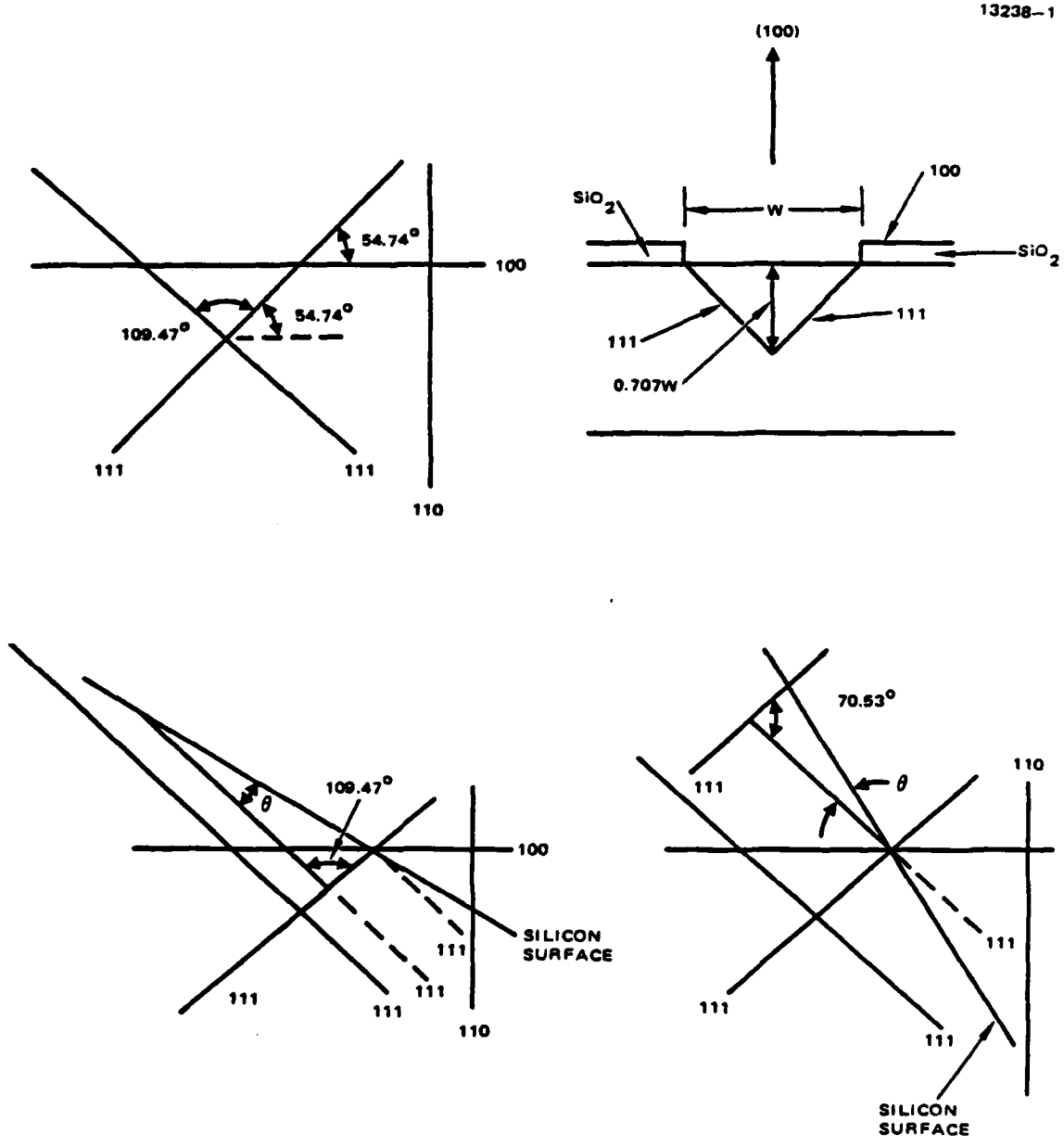

Figure 2. Anisotropic etch parameters for Si.

that if the correct etching time was chosen, the flat-top defect could be minimized, as shown in Figure 3. The excellent angle and groove shape control are clearly shown. Also seen is the slight undercut of the mask, due to the finite etching rate of the (111) planes.

We have procured a 2 in. diameter ingot that is being processed for slicing and polishing down to ~100 μm thickness. This is the thickness required to bend the grating to a 7.5 cm radius of curvature without breaking. We will fabricate 1.5 to 2.0 μm period gratings.

B. REPLICATED RULED GRATINGS

Although the silicon single-crystal grating approach is quite promising, we also started a series of experiments with replicated ruled gratings. Taking advantage of the high efficiency achievable with ruled, blazed planar gratings, we investigated the most suitable flexible substrate that will satisfy our needs.

Two types of replica gratings were obtained. The first type consists of a metallic grating replica layer supported only by a thin-film of epoxy resin. These very flexible gratings can easily be made to conform to the cylindrical curvature of the planar waveguide. But they are also very fragile and subject to distortion. As a result, the gratings exhibit phantom diffraction beams. When mounted in a Rowland configuration, we have observed an aberrated output spot. The distortion is mainly caused by wrinkles and air bubbles in the substrate and the stretching of epoxy resin.

Since this type of grating did not produce satisfactory results we decided to mount the grating on a semi-rigid substrate such as a cover glass. This was accomplished by hot-pressing the grating over the cover glass. We succeeded in getting a flat and smooth grating in some of the samples, but most showed poor surface quality due to air bubbles. It was

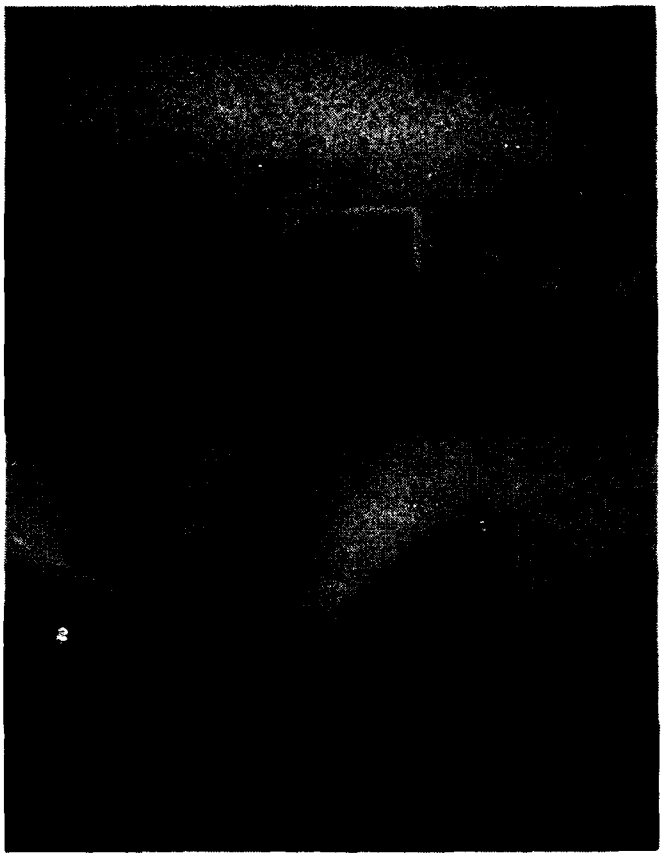

Figure 3. Short period grating in single crystal silicon with significantly reduced flat top defects.

decided to abandon this approach. Instead, we obtained from the vendor replica gratings which were supported by a thin, microscopic cover glass substrate. These gratings are rigid enough to provide the necessary flatness and yet flexible enough to bend and conform to the planar waveguide cylinder surface. We encountered some initial difficulties with a separation layer residue (see Figure 4) left on the grating replica by the manufacturer. A wash with warm distilled water removed this layer easily.

Gratings with glass substrates can be scribed and broken into long strips for testing. Typically, the diffraction efficiency was measured first in a planar grating configuration. The collimated output from a He-Ne laser or a semiconductor laser (0.82 μm and 1.3 μm) was directed to illuminate the grating at zero incident angle (the beam is perpendicular to the grating plane). Although the diffracted power was predominantly in one of the orders, several other orders were present as well. By summing the total diffracted power we determined that the grating had a total efficiency of ~80%. However, the main first order diffraction efficiency was ~70%. Several sets of readings were taken for different incident angles, with the efficiency changing only slightly with respect to the angle. We attached a number of grating strips on a planar waveguide developed for a previous program to examine the aberration performance. As expected, the output spot size depended critically on the accuracy of the grating curvature. Any deviation from the required curvature resulted in a much larger spot size as well as asymmetrical intensity distribution. These effects will certainly have an influence on the final device throughput loss and insertion loss performance. We also discovered that the present cover glass substrate was slightly too thick and the bent gratings occasionally snapped under pressure. We intend to search for a thinner glass substrate to alleviate this problem. The grating diffraction efficiency may still be improved by improving the grating surface quality, such

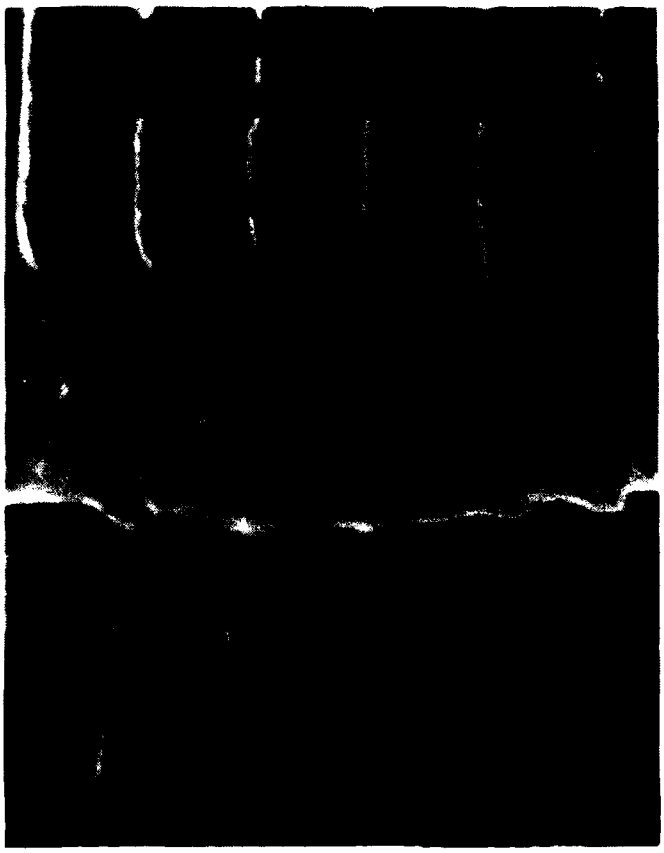

Figure 4. Separation layer residue on replica grating.

as by the complete removal of the separation layer and the use of sufficiently thick metallization (but not too thick to distort the blazed groove shape). Some of these improvements will require the cooperation of the manufacturer. Figure 5 shows the surface of a typical replica grating.

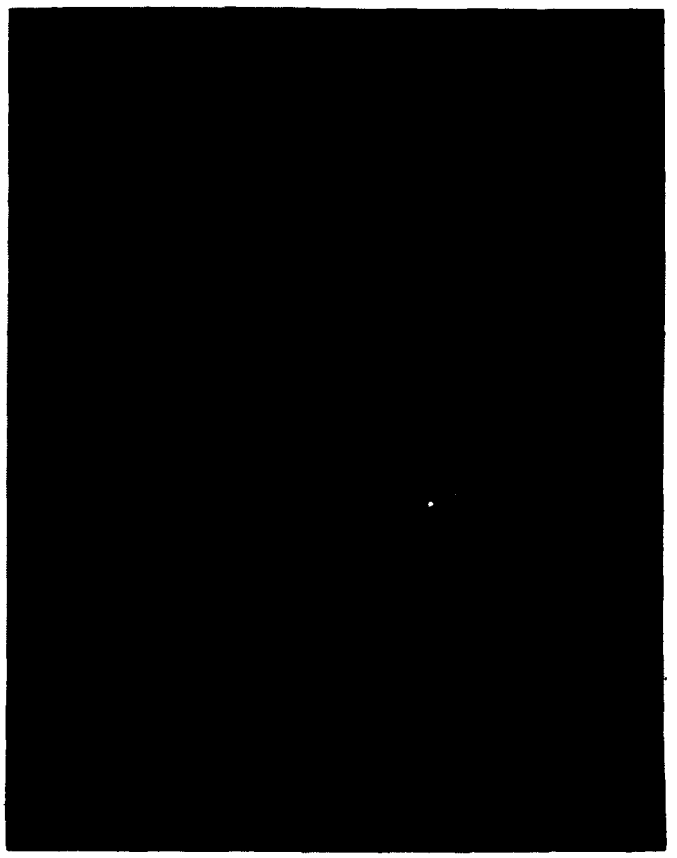

Figure 5. Surface of a replica grating.

SECTION III

FABRICATION OF PLANAR WAVEGUIDES

A. PLANAR WAVEGUIDE COMPONENT MATERIALS

To match a planar waveguide with a selected standard input and output fiber, the following materials properties must be specified and controlled:

Core Glass:	Index as close as possible to fiber core to keep Fresnel coupling losses to a minimum.
	Low absorption loss over wide near-IR wavelength region.
	Thermal coefficient of expansion to match cladding glass.
Cladding Glass:	Controlled index difference (~0.015) with core glass.
	Thermal coefficient of expansion to match core glass.
	Low absorption loss over wide near-IR wavelength region.
Bonding Cement:	100% solids content.
	Room temperature polymerizing.
	Lower index than core glass.
	Low absorption loss over wide near-IR wavelength region.
	Reliable glass bonder.
	High temperature softening point.

We have found that the choice of commercially available glasses and cements is limited. It was necessary to compromise on the materials specifications in order to implement the concept of an optimal planar waveguide for the Rowland coupler/decoupler at a reasonable cost.

As described in the semiannual report, our first set of planar waveguide glasses, Pair #1, consisted of a core of "High Reliability" Pyrex with an index of 1.4719 and a cladding of quartz with an index of 1.4588. This combination gave a waveguide numerical aperture of 0.2004 which matched the optical properties of the fiber perfectly but did not preserve the integrity of the thin core layer after lamination. "High Reliability" Pyrex has a thermal coefficient of expansion that is 2.7 X 10^{-6}/°C larger than that of quartz. Large tensile forces are generated during cooling after lamination and the thin core layer ruptures.

To reduce or eliminate this problem, we made a survey of commercially available optical glasses and correlated thermal coefficient of expansion with refractive index. The results of this survey are shown in Figure 6. This graph shows all pairs of interest, with a line connecting the two glass coordinates. It also shows numerical aperture for each pair and the thermal expansion coefficient mismatch and polarity. Compression of the core layer is shown by a positive value for the differential expansion coefficient. Desirable glass pairs have a numerical aperture close to 0.2 and place the core layer under slight compression.

We have chosen two new glasses for our experiments:

Pair #2: K10 Core Glass-FK5 Cladding Glass

This pair has a low numerical aperture value (0.2037) but has as very large compressive mismatch (+ 2.7 X 10^{-6}/°C).

Pair #3: K7 Core Glass-FK5 Cladding Glass

This pair has a larger numerical aperture than Pair #2 (0.2662), but has a smaller compressive mismatch (+ 8 X 10^{-7}/°C).

At the end of the program period reported here the glasses were received and plane polishing of the component plates was started.

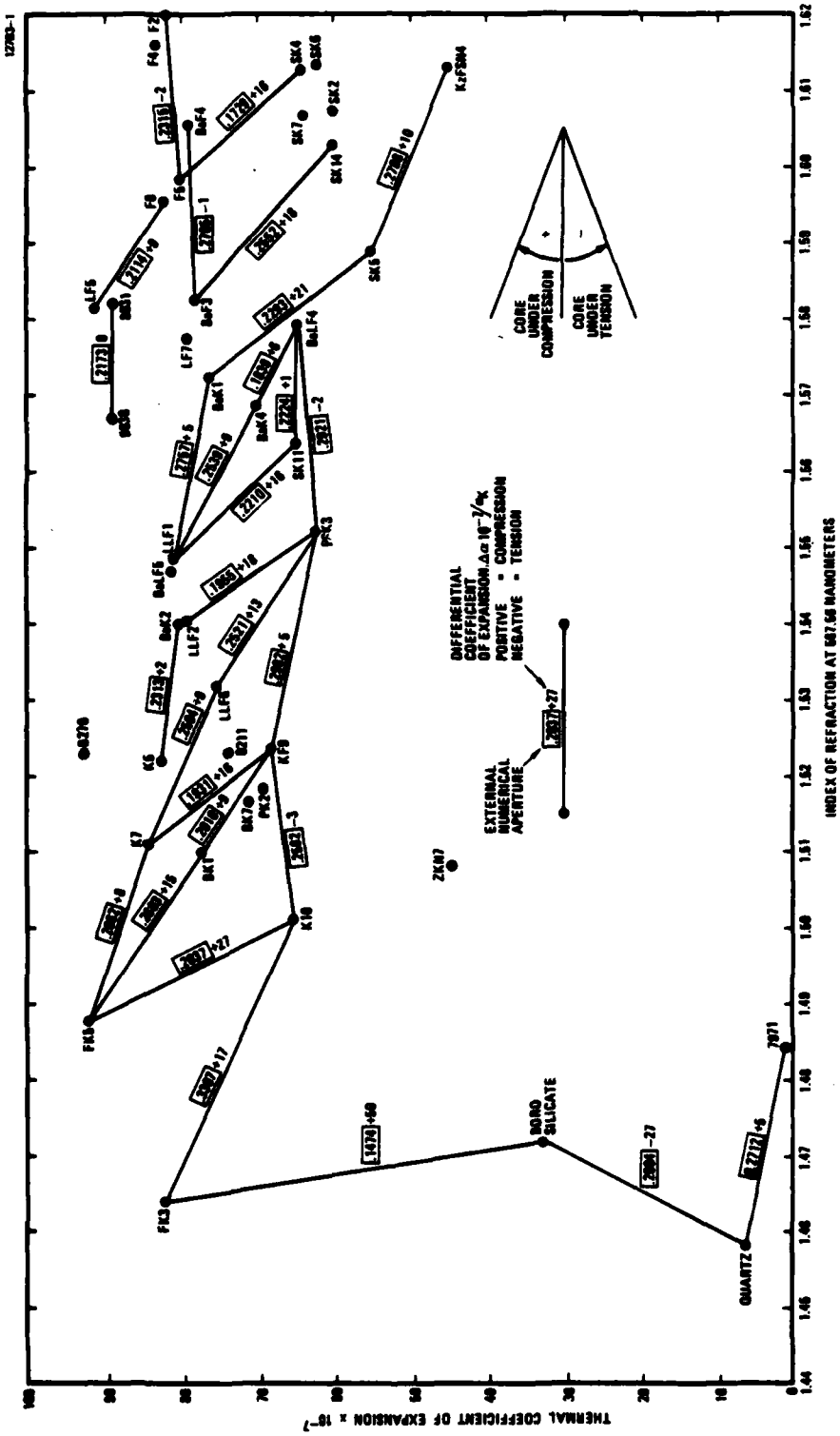

Figure 6. Correlation of glass properties for planar waveguides.

B. PLANAR WAVEGUIDE ASSEMBLY PROCESS

Pending the success of a Hughes-sponsored search for a room-temperature, photopolymerizable, low refractive index optical bonding cement, our present work continues to rely on the TPX hot-melt laminating process developed for this program. A patent disclosure on this process has been written and had been rated for filing by the HRL Patent Review Committee.

Figure 7 shows the process flow chart and the steps leading to a complete waveguide sandwich. The glass layers are laminated to hot melted sheets of polymethylpentene (TPX) with the aid of the proprietary adhesion promoting process. Using this process and assuming optically flat interfaces, an assemblied planar waveguide sandwich can be made in two ways:

1. Laminating with thin (<2-μm-thick) glue line

The thin glue line has negligible effect on the numerical aperture of the planar waveguide and the index difference between the core and the cladding glass determines the numerical aperture. Absorption losses are determined by properties of the core and the cladding glass.

2. Laminating with thick (~10-μm-thick) glue line

The bonding glue layer acts as the cladding for the core glass and the waveguide numerical aperture is determined by the index difference between the core glass and the laminating glue. Optical absorption of the glue affects losses. Core glass and cladding glass can be identical, eliminating the thermal coefficient mismatch problem.

For method #1, we must develop a process for "wringing out" excess glue and reducing the thickness of the glue line.

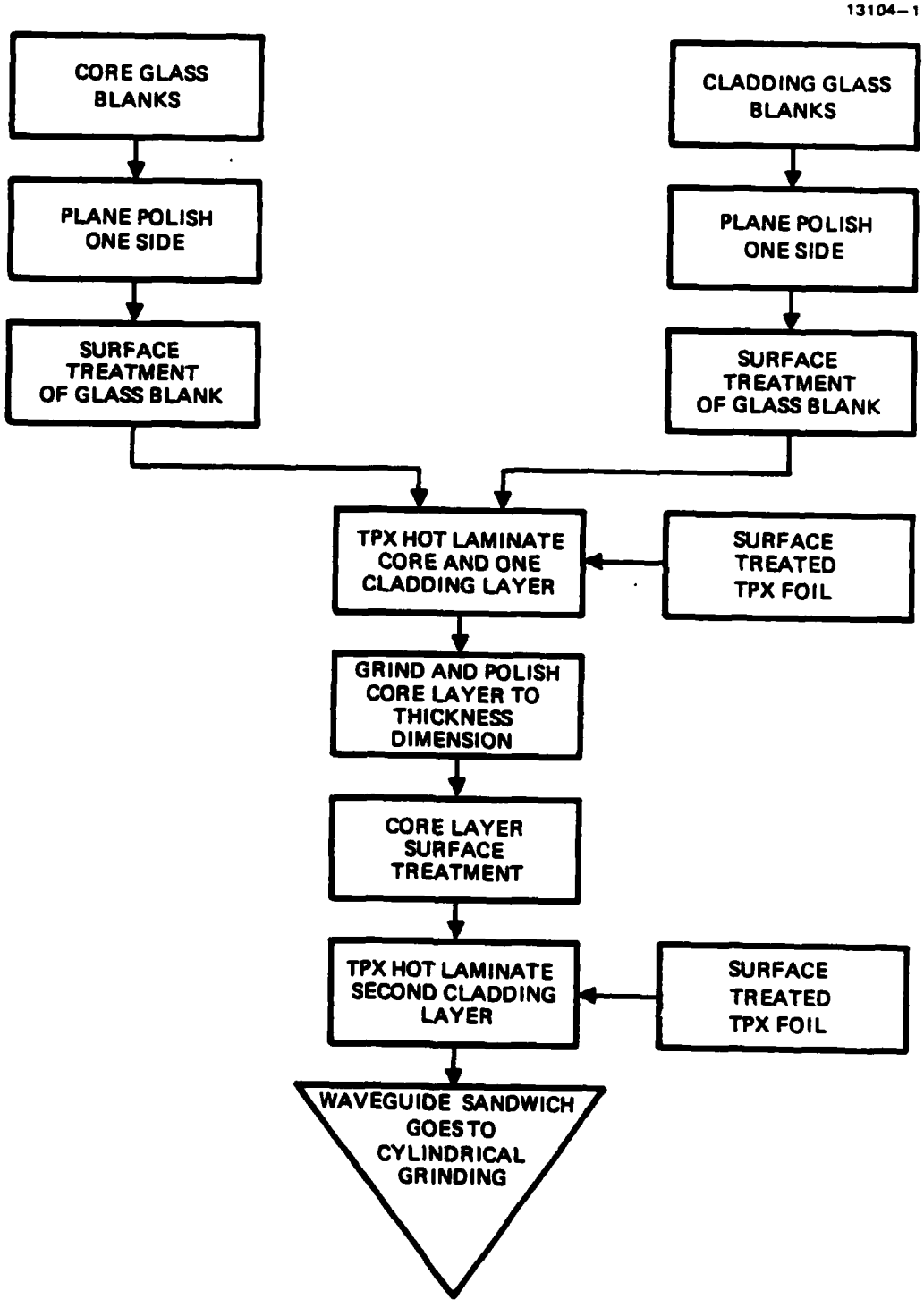

Figure 7. Process flow diagram (partial) for planar waveguide preparation.

For method #2, we must find out whether the absorption losses of the cement are low enough to make this approach viable.

To date, no complete three-layer planar waveguide sandwich that has a low numerical aperture and that matches a standard fiber has been assembled. All prior work faltered at the two-layer assembly stage. With the new glasses we expect to overcome the difficulties caused by thermal coefficient of expansion mismatch.

SECTION IV

CONCLUSIONS AND RECOMMENDATIONS

The contract specified in the general requirements section (3.2) that: "EACH MEMBER OF THE COUPLER/DECOUPLER FAMILY SHALL BE CAPABLE OF COUPLING ONTO, AND DECOUPLING OFF OF, AN OPTICAL TRANSMISSION LINE...", imposing the design requirements for the miniature Rowland coupler/decoupler.

The coupler/decoupler must be able to operate into and out of a single system-wide type of optical fiber with standardized étendue (core diameter and numerical aperture) for both input and output.

Coupler/decouplers of the prior art employed large numerical apertures and large core layer thickness structures in order to assure collection of all the fiber radiant flux at the input end. This forces the designers to use larger diameter fibers and/or larger numerical aperture fibers at the output end.

The need of the present contract (ibid.) that ..."THE FAMILY OF COUPLERS SHALL UTILIZE COMMON COMPONENTS"...and that ..."MODULES OF A GIVEN TYPE SHALL BE INTERCHANGEABLE AND INTEROPERABLE WITH OTHER TYPES OF MODULES"...establishes the need for a planar waveguide structure matching both the core dimension and numerical aperture of the interconnecting standard fibers.

This is the technical problem which proves to be more difficult to solve than was anticipated at the start of the program. We know how to control the dimensions of the core layer, but control of the planar waveguide numerical aperture requires selection of glasses and bonding cements with unusual combinations of properties.

We have found the first solution to the low index cement problem, and, instead of having special custom glasses prepared (a costly and time-consuming process beyond the scope of this

program), we have chosen to use commerically available glasses with near approximate optical and thermomechanical properties.

In the coming months we will assemble complete (three-layer) waveguides using commercially available glasses and using the TPX hot-melt laminating process. The thermal stability of the assembly will be investigated to ensure mechancial integrity. Cyclindrical end surfaces will then be ground and polished on the three-layer sandwiches and the flexible grating will be attached.

To investigate some peripheral aspects of this program we used Hughes IR&D funds for an early part of a study into holographically exposed, anisotropically etched single-crystal silicon gratings, and for a small study of synthetic processes to prepare low refractive index glass-bonding cements.

REFERENCES

1. S. Sriram et al., "Fiber Coupled Tapered Channel Waveguide Array," Cleo 5, 1980, Paper #WCC2.

2. T. Kita et al., "Use of Aberration Corrected Concave Gratings in Optical Demultiplexers," Appl. Opt. 22, 819, (1983).

3. Y. Fujii et al., "Optical Demultiplexer Using A Silicon Concave Diffraction Grating," Appl. Opt. 22, 974, (1983).

4. Master Glass Catalogs of Schott Glass, Corning Glass, Corning France, Hoya Glass and Ohara Glass.

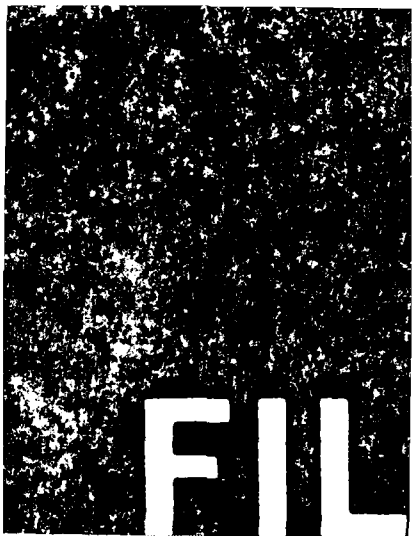
FIL